RSC Advances

PAPER

View Article Online
View Journal | View Issue

Cite this: *RSC Adv.*, 2017, **7**, 7217

Six new coordination compounds based on rigid 5-(3-carboxy-phenyl)-pyridine-2-carboxylic acid: synthesis, structural variations and properties†

Jiang-Feng Song,*[a] Ying-Ying Jia,[a] Rui-Sha Zhou,[a] Si-Zhe Li,[a] Xiao-Min Qiu[a] and Jie Liu*[b]

Six new coordination compounds Ni(cppca)$(H_2O)_4\cdot 2H_2O$ (**1**), Co(cppca)$(H_2O)_4\cdot 2H_2O$ (**2**), $\{Cd_2(cppca)_2(H_2O)_5\}_n$ (**3**), $\{[Cd_3(cppca)_2(H_2P_2O_7)(H_2O)_6]\cdot 2H_2O\}_n$ (**4**), $\{Cu(Hcppca)_2\}_n$ (**5**) and $\{[Mn_7(cppca)_6(Hcppca)_2(H_2O)_{10}]\cdot 2H_2O\}_n$ (**6**) have been obtained by reactions of the corresponding metal salts and the rigid ligand 5-(3-carboxy-phenyl)-pyridine-2-carboxylic acid (H_2cppca) under solvothermal conditions. All the compounds were fully characterized by single-crystal X-ray diffraction, elemental analysis, IR spectroscopy, thermal analysis and powder X-ray diffraction. The single-crystal X-ray analyses showed that compounds **1–6** have rich structural chemistry ranging from mononuclear (**1** and **2**), one-dimensional (**3** and **4**), two-dimensional (**5**) to three-dimensional (**6**) structures. Moreover, the framework of compound **6** may be simplified into a 3-nodal net with Schlafli symbol $\{4^2\cdot 6\}\{4^2\cdot 8^2\cdot 10^2\}\{4^3\cdot 6^2\cdot 8\cdot 10^4\}_2$, which shows an unprecedented (3,4,5)-connected topology net. The fluorescent properties of compounds **3** and **4** were investigated in the solid state and in various solvent emulsions, which indicated that compounds **3** and **4** are both highly sensitive fluorescent probes for the acetone molecules. Variable-temperature magnetic susceptibility measurements indicate weak antiferromagnetic interactions between metal centers in compounds **1**, **2**, **5** and **6**.

Received 18th November 2016
Accepted 16th January 2017

DOI: 10.1039/c6ra26966d

www.rsc.org/advances

Introduction

Coordination compounds have attracted considerable attention due to their intriguing structures[1] and wide potential applications in gas storage and separation,[2] luminescence,[3] molecular magnetism,[4] catalysis,[5] *etc.* Although lots of effort has been put into developing the ability to control the reactions, and significant progress has also been made, the controllable synthesis of coordination compounds with unique structure and function still remains a long-term challenge because their self-assembly processes are often influenced by compositional (chemical structure of ligands chosen, kind of metal salt, pH value, solvent system, metal-to-ligand ratio, *etc.*) and process parameters (reaction time, temperature, and pressure).[6]

As is well known, the selection and design of proper organic ligands have a large impact on the construction of coordination compounds with novel structures and unique properties. Among the chosen ligands, N-heterocyclic carboxylates have been widely used to construct coordination compounds due to their multiplicity of coordinated atoms and wide range of binding modes resulting in good ligating ability to metal ions in various arrangements.[7] To date, diverse complexes based on N-heterocyclic carboxylates such as imidazole-carboxylic acid,[8] pyridine-carboxylic acid,[9] pyrimidine-carboxylic acid,[10] and so on, have been reported, which possess intriguing topology structures and specific functional characteristics. Here, the conjugated N-heterocyclic dicarboxylic ligand, 5-(3-carboxy-phenyl)-pyridine-2-carboxylic acid (H_2cppca), is introduced as a rigid linker for the reasons as follows: (i) it possesses four carboxylic oxygen atoms and one pyridyl nitrogen atom, which can assume many kinds of bridging or chelating modes to meet the geometric coordination requirement of metal centers. (ii) The H_2cppca ligand might be partially or completely deprotonated at different pH values to adopt various acidity-dependent binding modes, on the other hand, it can act as hydrogen bond acceptors and donors to benefit the formation of various supramolecular structures.[11] (iii) The flexible C–C single bonds between phenyl and pyridyl rings can rotate freely, as results in the formation of *cis*- and *trans*-conformations and enrich structures of coordination compounds. (iv) The conjugated phenyl and pyridyl system of the H_2cppca ligand is helpful to provide remarkable luminescent performances and stable architecture.[12] Based on the above mentioned analysis, the H_2cppca ligand should be an effective component in the design of functional coordination complexes.

[a]*Department of Chemistry, North University of China, Taiyuan, Shanxi, 030051, P. R. China. E-mail: jfsong0129@nuc.edu.cn*

[b]*State Key Laboratory of Polymer Physics and Chemistry, Changchun Institute of Applied Chemistry, Chinese Academy of Sciences, Changchun, 130022, P. R. China. E-mail: liujie@ciac.ac.cn*

† Electronic supplementary information (ESI) available: Table S1, Fig. S1–S5 and X-ray crystallographic files in CIF format of compounds **1–6**. CCDC 1509277–1509282. For ESI and crystallographic data in CIF or other electronic format see DOI: 10.1039/c6ra26966d

Herein, we describe the design and synthesis of six new coordination compounds based on H_2cppca, Ni(cppca)$(H_2O)_4\cdot 2H_2O$ (**1**), Co(cppca)$(H_2O)_4\cdot 2H_2O$ (**2**), $\{Cd_2(cppca)_2(H_2O)_5\}_n$ (**3**), $\{[Cd_3(cppca)_2(H_2P_2O_7)(H_2O)_6]\cdot 2H_2O\}_n$ (**4**), $\{Cu(Hcppca)_2\}_n$ (**5**), $\{[Mn_7(cppca)_6(Hcppca)_2(H_2O)_{10}]\cdot 2H_2O\}_n$ (**6**). All the compounds were fully characterized by single-crystal X-ray diffraction, elemental analysis, IR spectroscopy, thermal analysis and powder X-ray diffraction. The fluorescence properties of compounds **3** and **4** in the solid state and in various solvent emulsions have also been investigated, displaying highly sensitive fluorescent probes for the acetone molecules. The magnetic properties of compounds **1**, **2**, **5** and **6** have been investigated.

Experimental

Materials and physical measurements

All reagents and solvents were commercially available and used as received without further purification. Elemental analysis (C, H, and N) was performed on a Perkin-Elmer 240C elemental analyzer. Infrared (IR) spectra were obtained with KBr Pellets on a Perkin Elmer Spectrum One FTIR spectrometer in the range of 4000–400 cm^{-1} with the resolution (4.0 cm^{-1}) and the scan's numbers.[10] Powder X-ray diffraction (PXRD) patterns of the samples were recorded by a RIGAKU-DMAX2500 X-ray diffractometer using Cu-Kα radiation (λ = 1.542 Å) with a scanning rate of 10° min^{-1} and a step size of 0.02°. Thermalgravimetric analysis (TGA) was performed on a Perkin-Elmer TGA-7000 thermogravimetric analyzer with a heating rate of 10 °C min^{-1}. The solvent emulsion and solid fluorescent spectra of compounds **3** and **4** were obtained on a HITACHI F-2700 fluorescence Spectrophotometer at room temperature. Variable-temperature magnetic susceptibility measurements were collected using SQUID magnetometer MPMS XL-7 (Quantum Design) at 1.0 kOe in the temperature range of 2–300 K.

Synthesis of compounds 1–6

Synthesis of $\{Ni(cppca)(H_2O)_4\cdot 2H_2O\}_n$ (1). A mixture of $NiCl_2\cdot 6H_2O$ (0.1 mmol) and H_2cppca (0.05 mmol) was dissolved in a DMF/H_2O solution (v/v = 3 : 3, 6 mL), which was sealed in a 20 mL Teflon-lined stainless-steel reactor, heated at 80 °C for 72 h under autogenous pressure. After slowly cooling to room temperature, green stick crystals of compound **1** were collected by filtration and washed with distilled water several times. Yield: 60% (based on the H_2cppca). Elemental anal. calcd $C_{13}H_{19}NNiO_{10}$ (408): C, 38.24; H, 4.66; N, 3.43. Found: C, 38.25; H, 4.65; N, 3.45. IR data (KBr, cm^{-1}): 3358(s), 3174(s), 1618(s), 1543(s), 1383(s), 1255(m), 881(m), 759(m).

Synthesis of $\{Co(cppca)(H_2O)_4\cdot 2H_2O\}_n$ (2). The procedure was the same as that for compound **1** except that $NiCl_2\cdot 6H_2O$ (0.1 mmol) was replaced by $Co(Ac)_2\cdot 6H_2O$ (0.1 mmol). Pink acicular crystals of compound **2** were collected in 52% yield (based on the H_2cppca). Elemental anal. calcd $C_{13}H_{19}CoNO_{10}$ (408.22): C, 38.21; H, 4.65; N, 3.43. Found: C, 38.25; H, 4.65; N, 3.42. IR data (KBr, cm^{-1}): 3358(s), 3174(s), 1618(s), 1543(s), 1383(s), 1255(m), 881(m), 759(m).

Synthesis of $\{Cd_2(cppca)_2(H_2O)_5\}_n$ (3). The procedure was the same as that for compound **1** except that $NiCl_2\cdot 6H_2O$ (0.1 mmol) was replaced by $CdCl_2\cdot 6H_2O$ (0.1 mmol). Colorless crystals of compound **3** were collected in 55% yield (based on the H_2cppca). Elemental anal. calcd $C_{26}H_{24}Cd_2N_2O_{13}$ (797.31): C, 39.13; H, 3.01; N, 3.51. Found: C, 39.10; H, 3.03; N, 3.50. IR data (KBr, cm^{-1}): 3417(s), 3174(s), 1626(m), 1556(s), 1391(s), 1028(m), 871(m), 771(m).

Synthesis of $\{[Cd_3(cppca)_2(H_2P_2O_7)(H_2O)_6]\cdot 2H_2O\}_n$ (4). A mixture of $CdCl_2\cdot 6H_2O$ (0.1 mmol), H_2cppca (0.05 mmol) and DMF/H_2O/MeOH (3 : 1 : 3, 7 mL) was stirred in a 25 mL beaker for 5 minutes at room temperature. The above-mentioned mixtures, in which pyrophosphate aqueous solution (0.1 mL, 0.1 mol L^{-1}) was added, were transferred and sealed in a 20 mL Teflon-lined stainless steel reactor and kept under autogenous pressure at 80 °C for 72 h. After slowly cooling to room temperature, light-yellow block crystals were obtained and washed with distilled water. Yield: 43% (based on the H_2cppca). Elemental anal. calcd $C_{26}H_{32}Cd_3N_2O_{23}P_2$ (1139.68): C, 27.38; H, 2.81; N, 2.46. Found: C, 27.42; H, 2.79; N, 2.50. IR data (KBr, cm^{-1}): 3408(s), 1608(m), 1548(s), 1399(s), 1092(s), 871(m), 771(m).

Synthesis of $\{Cu(Hcppca)_2\}_n$ (5). H_2cppca (0.05 mmol) and $CuCl_2\cdot 4H_2O$ (0.05 mmol) were mixed in CH_3CN/H_2O (4 : 4, 8 mL) solutions, and stirred for 0.5 h, then the mixture was transferred into a 20 mL Teflon-lined stainless steel container and heated at 150 °C for 72 h. After slowly cooling to room temperature, blue block crystals of compound **5** were isolated and washed with distilled water. Yield: 33% (based on the H_2cppca). Elemental anal. calcd $C_{26}H_{16}CuN_2O_8$ (547.95): C, 56.94; H, 2.92; N, 5.11. Found: C, 56.95; H, 2.90; N, 5.09. IR data (KBr, cm^{-1}): 3438(m), 1684(s), 1612(s), 1377(m), 1249(m), 759(m).

Synthesis of $\{[Mn_7(cppca)_6(Hcppca)_2(H_2O)_{10}]\cdot 2H_2O\}_n$ (6). A mixture of $MnCl_2\cdot 4H_2O$ (0.05 mmol), H_2cppca (0.05 mmol) and CH_3CN/H_2O (4 : 4, 8 mL) was stirred for 0.5 h to form a suspension where NaOH (0.1 M) was added to adjust pH = 6.0. Then the suspension was sealed in a 20 mL Teflon-lined stainless steel container and heated at 120 °C for 72 h. After slowly cooling to room temperature, light-yellow rod crystals of compound **6** were isolated after washed with water several times. Yield: 35% (based on the H_2cppca). Elemental anal. calcd $C_{104}H_{80}N_8O_{44}Mn_7$ (2530.34): C, 49.32; H, 3.16; N, 4.43. Found: C, 46.35; H, 3.12; N, 4.45. IR data (KBr, cm^{-1}): 3438(m), 1626(m), 1556(s), 1385(s), 1191(m), 1028(m), 764(m).

Single crystal structure determination

The crystal structures were determined by single-crystal X-ray diffraction. Reflection data were collected on a Bruker SMARTCCD area-detector diffractometer (Mo-Kα radiation, graphite monochromator) at room temperature with ω-scan mode. Empirical adsorption correction was applied to all data using SADABS. The structure was solved by direct methods and refined by full-matrix least squares on F^2 using SHELXTL 97 software.[13] Non-hydrogen atoms were refined anisotropically. All C-bound H atoms were refined using a riding model. All

Table 1 Crystal data and structure refinement information for compounds **1–6**

Compound	**1**	**2**	**3**	**4**	**5**	**6**
Empirical formula	$C_{13}H_{19}NNiO_{10}$	$C_{13}H_{19}CoNO_{10}$	$C_{26}H_{24}Cd_2N_2O_{13}$	$C_{26}H_{32}Cd_3N_2O_{23}P_2$	$C_{26}H_{16}CuN_2O_8$	$C_{104}H_{82}Mn_7N_8O_{44}$
Formula weight	408.00	408.22	797.27	1131.70	547.95	2532.36
Crystal system	Monoclinic	Monoclinic	Triclinic	Monoclinic	Monoclinic	Triclinic
Space group	$P2_1/c$	$P2_1/c$	$P\bar{1}$	$C2/c$	$P2_1/c$	$P\bar{1}$
a/Å	15.569(3)	15.5726(4)	7.7894(16)	35.360(7)	8.3091(6)	13.136(3)
b/Å	7.7545(16)	7.7978(2)	12.085(2)	11.899(2)	7.1846(6)	14.882(3)
c/Å	13.712(3)	13.7900(5)	14.169(3)	7.9016(16)	19.0036(14)	15.283(3)
α/°	90.00	90.00	82.94(3)	90.00	90.00	116.26(3)
β/°	99.11(3)	98.943(3)	81.63(3)	90.88(3)	98.168(7)°	93.42(3)
γ/°	90.00	90.00	89.49(3)	90.00	90.00	108.77(3)
V/(Å^3)	1634.5(6)	1654.19(8)	1309.5(5)	3324.2(12)	1122.96(15)	2464.2(9)
Z	4	4	2	4	2	1
ρ_{calc}/g cm^{-3}	1.658	1.639	2.022	2.261	1.621	1.706
Absorption coef.	1.242	1.092	1.701	2.097	1.031	0.973
Reflns collected	15 359	7682	12 699	15 602	3876	19 497
Unique reflns (R_{int})	3728(0.0288)	2955(0.0335)	5922(0.0208)	3788(0.0423)	1995(0.0203)	8673(0.0317)
Completeness	99.7%	99.9%	98.6%	99.0%	99.8%	98.6%
GooF	1.227	1.099	1.179	1.075	1.095	1.066
R_1, wR_2 [$I > 2\sigma(I)$][a]	0.0330, 0.0854	0.0339, 0.0727	0.0250, 0.0675	0.0629, 0.1801	0.0370, 0.0821	0.0402, 0.0980
R_1, wR_2 (all data)	0.0400, 0.0954	0.0428, 0.0776	0.0322, 0.0819	0.0736, 0.1867	0.0484, 0.0902	0.0550, 0.1030

[a] $R_1 = \Sigma||F_o| - |F_c||/\Sigma|F_o|$; $wR_2 = [\Sigma w(F_o^2 - F_c^2)_2/\Sigma w(F_o^2)^2]^{1/2}$.

calculations were carried out using SHELXTL 97. The crystallographic data and pertinent information for compounds **1–6** are contained in Table 1; selected bond lengths and angles are listed in Table S1.†

Results and discussion

Synthesis of compounds 1–6

Due to the rigid structure of the H_2cppca ligand, the mixture of metal salt and organic ligand in different solvents usually produced lots of precipitations at room temperature, as makes the crystal complexes difficultly to be obtained, so compounds **1–6** were synthesized under the solvothermal conditions. DMF or acetonitrile is helpful to solve the H_2cppca ligand, as provides a facility for the solvothermal reactions. The experimental results indicate that the reaction solvents and temperature play an important role in the preparation of compounds **1–6**. Compounds **1–3** were obtained with high yield by the solvothermal reaction of metal ions and H_2cppca in a DMF/H_2O solution, however, DMF was substituted by the other organic solvents such as methanol, ethanol, acetonitrile, *etc.*, crystalline compounds **1–3** were difficult to be synthesized. Compound **4** has been obtained through adding pyrophosphoric acid methanol solution to DMF/H_2O (3 : 3) solutions, methanol was crucial for the synthesis of compound **4**, small crystals of compounds **4** were obtained if methanol was absent in the reaction. Notably, very small crystals of compounds **5** and **6** were obtained when the reaction solvent is DMF/H_2O solutions, while DMF was substituted by CH_3CN and further increased the reaction temperature, compounds **5** and **6** with larger crystals were obtained successfully, because high temperature and the pressure during the reaction process are helpful to improve the ligand solubility and enhance the reactivity of reactant.

Crystal structures of{Ni(cppca)$(H_2O)_4\cdot 2H_2O$}$_n$ (1) and {Co(cppca)$(H_2O)_4\cdot 2H_2O$}$_n$ (2). Compounds **1** and **2** with different molecular formula have the same crystal system, space group and isomorphic frameworks, so only the structure of compound **1** has been described in detail as a representative example. The single-crystal X-ray diffraction analysis reveals that compound **1** crystallizes in monoclinic space group $P2_1/c$. As shown in Fig. 1a, compound **1** is a mononuclear complex in which the central Ni atom with a slightly distorted octahedral geometry receives contributions from five oxygens and one nitrogen belonging to one cppca^{2-} anion and four water molecules. The cppca^{2-} anion coordinates with Ni(II) in an N,O-chelating mode: μ_1-κN,O (Fig. 2a). The Ni–N/O distances are in the range of 2.0375(18)–2.0946(18) Å, and the O/N–Ni–O/N bond angles range from 80.27(7) to 177.75(7)°.

Two Ni$(H_2O)_4$ units constructed by the Ni center and four coordinated water are interconnected into a $Ni_2(H_2O)_8$ dimer

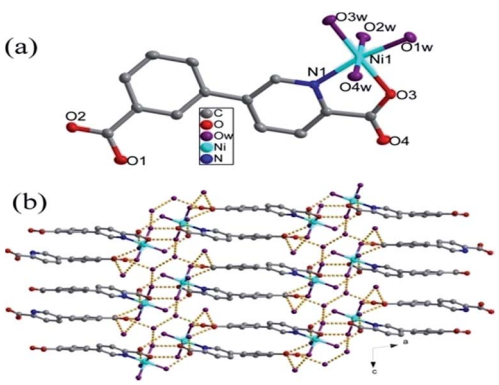

Fig. 1 (a) Coordination environment of the Ni(II) ion, the hydrogen atoms are omitted for clarity. (b) The 3D supramolecular network in compound **1**.

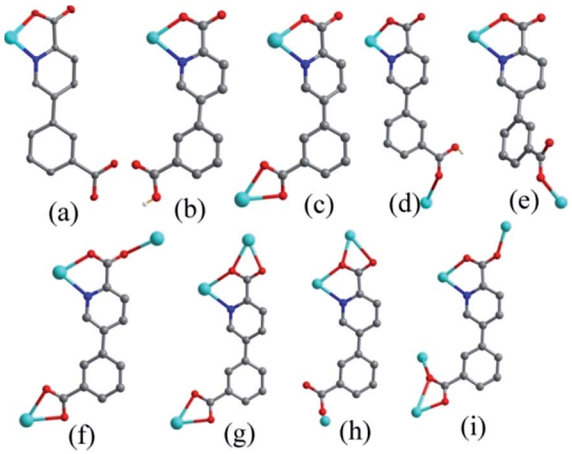

Fig. 2 Coordination modes of the H_2cppca ligands in compounds 1–6.

with six-membered ring through O1w–H···O4w hydrogen bonds (Fig. S1†). In $Ni_2(H_2O)_8$ dimer, coordinated O1w and O4w interact with lattice water molecules (O5w and O6w) *via* hydrogen bonds, respectively; there are two hydrogen bonds between coordinated O2w and lattice water molecules (O5w and O6w). The interactions between $Ni_2(H_2O)_8$ dimers and lattice water molecules (O5w and O6w) result in the formation of a rather complex 2D supramolecular layer *via* hydrogen bonds, in which O5w and O6w bridge two dimmers (Fig. S2†). The 2D supramolecular layers were joined into a 3D supramolecular network through O–H···O hydrogen bonds between uncoordinated carboxyl group of $cppca^{2-}$ anions and water molecules (Fig. 1b).

Crystal structures of $\{Cd_2(cppca)_2(H_2O)_5\}_n$ (3). A single-crystal X-ray diffraction shows that compound **3** crystallizes in the triclinic space group $P\bar{1}$. The asymmetric unit of **3** contains two Cd^{2+} ions, two $cppca^{2-}$ anions, and five coordination water molecules (Fig. 3a). The Cd_1 center with a slightly distorted pentagonal bipyramid geometry where the equatorial plane comprises four carboxylate O atoms (O2, O5, $O3^{ii}$ and $O4^{ii}$) and one N atom (N1) from three different $cppca^{2-}$ anions, and two water molecules (O1w and O2w) occupy the apical sites. Similar with Cd_1, Cd_2 is bound to six oxygens and one nitrogen from two independent $cppca^{2-}$ anions and three water molecules. The Cd–N/O bond lengths are 2.275(3) and 2.434(3) Å, and the O/N–Cd–O/N bond angles range from 53.77(9) to 172.25(13)°.

In compound **3**, two different coordination modes of $cppca^{2-}$ anions are observed in the completely deprotonated $cppca^{2-}$ ligands: μ_2-κN,O:κO′,O″ (Fig. 2c) and μ_3-κO:κN,O:κO′,O″ (Fig. 2f). Two symmetry-related Cd_1 metal centers are connected into a 18-membered ring by two $cppca^{2-}$ ligands adopting μ_2 coordination modes (abbreviated to Ring A). Interestingly, another 18-membered ring is composed of two Cd_2 centers and two $cppca^{2-}$ ligands adopting μ_3 coordination modes (abbreviated to Ring B). Each Ring B joins two Ring A into an extended 1D chain *via* Cd–O bonds (Fig. 3b).

Crystal structures of $\{[Cd_3(cppca)_2(H_2P_2O_7)(H_2O)_6]\cdot 2H_2O\}_n$ (4). A single-crystal X-ray diffraction shows that compound **4** crystallizes in the monoclinic space group *C*2/*c*. The asymmetric unit of **4** contains one and a half Cd^{2+} ions, one $cppca^{2-}$ ligand, half a $[H_2P_2O_7]^{2-}$ anion, three coordinated and one lattice water molecules. As depicted in Fig. 4a, both Cd centers in compound **4** are seven-coordinated and adopt a slightly distorted pentagonal bipyramid geometry. The Cd_1 center coordinating with four carboxyl oxygen atoms (O1, O2, $O1^i$, and $O2^i$) from two different $cppca^{2-}$ ligands and one oxygen atom (O5) from $[H_2P_2O_7]^{2-}$ anion in the equatorial positions, and two symmetry-related coordinated water molecules occupy the apical positions. While the Cd_2 center is bound to six oxygens and one nitrogen from two independent $cppca^{2-}$ anions, one coordinated $[H_2P_2O_7]^{2-}$ anion and two water molecules. The Cd–O/N bond distances are in the range of 2.255(9)–2.458(6) Å and the O/N–Cd–O/N bond angles range from 54.3(2) to 178.9(4)°.

The $cppca^{2-}$ adopting μ_3-κN,O:κO′,O″:κO,O‴ coordination mode (Fig. 2g) and $[H_2P_2O_7]^{2-}$ anions each connect two Cd_1 and one Cd_2 centers into a bent Cd_3 secondary building units (SBUs). The Cd_3 SBUs are further joined into a 1D chain by four $cppca^{2-}$ anions, in which there exist in an 18-membered ring constructed by two $cppca^{2-}$ ligands and two Cd_2 centers (Fig. 4b).

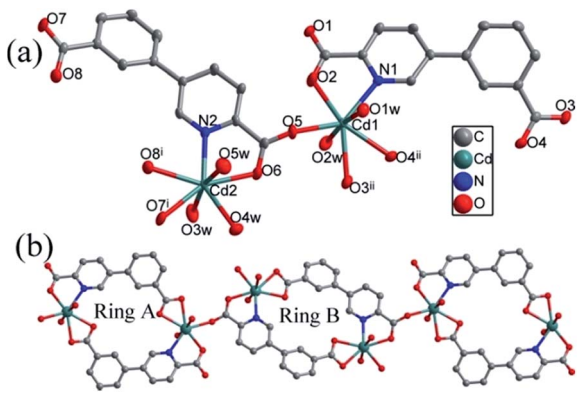

Fig. 3 (a) Coordination environment of the Cd(II) ions. The hydrogen atoms are omitted for clarity. (b) The 1D chain constructed by Ring A and Ring B in compound **3**.

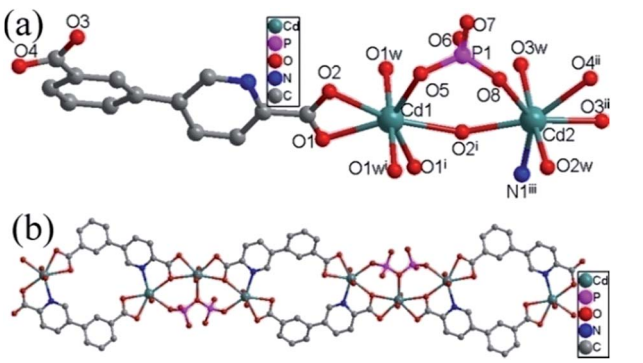

Fig. 4 (a) Coordination environment of the Cd(II) ions. The hydrogen atoms are omitted for clarity. (b) The 1D chain in compound **4**.

Crystal structures of $\{Cu(Hcppca)_2\}_n$ (5). Compound **5** crystallizes in monoclinic space group $P2_1/c$. The asymmetric unit is composed of half a Cu(II) center and one partially deprotonated $(Hcppca)^-$ anion (Fig. 5a). The Cu center with a slightly distorted octahedral geometry where the basal plane occupied by two carboxylate O atoms (O4 and O4^{iii}) and two N atoms (N1 and N1^{iii}) from two chelating $(Hcppca)^-$ ligands, lies on a crystallographic inversion center, and the axes are occupied by two carboxylate oxygen atoms from another two $(Hcppca)^-$. The Cu–O/N bond distances are in the range of 1.930(2)–2.564 Å, obviously, the Cu–O distances (2.564 Å) in axes are longer than that of the basal plane due to Jahn–Teller distortion. Each $(Hcppca)^-$ anion connects two Cu(II) ions to generate a 2D layer in μ_2-κN,O:κO′ coordination mode (Fig. 2d), in which 1D left- and right-handed helical chains with the Cu···Cu separation of 7.1846 Å alternately arrayed (Fig. 5b).

Crystal structures of $\{[Mn_7(cppca)_6(Hcppca)_2(H_2O)_{10}]\cdot 2H_2O\}_n$ (6). Compound **6** crystallizes in triclinic space group $P\bar{1}$. The asymmetric unit of compound **6** contains four crystallographically independent manganese(II) ion (Mn_1, Mn_2, Mn_3 and Mn_4), three $cppca^{2-}$ anions, one $(Hcppca)^-$ anion, five coordinated and one lattice water molecules (Fig. 6a). Mn_1 is six-coordinated with six oxygens from four $cppca^{2-}$ anions and two water molecules, forming a distorted octahedral geometry. Mn_2 with octahedral geometry is bound to three carboxylate oxygens and two nitrogens from two independent $cppca^{2-}$ and one $(Hcppca)^-$ anions and one oxygen from a water molecule, similar with Mn_2, Mn_4 also coordinates with four oxygens and two nitrogens from three independent $cppca^{2-}$ anions and one water molecule. While Mn_3 exhibits a slightly distorted trigonal bipyramidal geometry, which is bound to five oxygens from three different $cppca^{2-}$ anions and two coordination water molecule. The Mn–O/N bond distances around Mn centers are in the range of 2.119(2)–2.284(3) Å, and the O/N–Mn–O/N bond angles range from 72.64(8) to 180.00(1)°.

Interestingly, there exist in four types of coordination modes for organic linker: μ_1-κN,O; μ_2-κN,O:κO′; μ_4-κN,O:κO,κO′:κO″ and μ_4-κN,O:κO′:κO″:κO‴ fashions (Fig. 2b, e, h, i). Mn_2, Mn_3 and Mn_4 are assembled into a linear Mn_3 secondary building unit (SBU) by carboxyl groups from $cppca^{2-}$ anions. The Mn_3 SBUs are joined into a 1D chain by $cppca^{2-}$ anions adopting μ_4-κN,O:κO,κO′:κO″ coordination mode, in which an 18-membered ring constructed by two $cppca^{2-}$ ligands and two Mn centers (Fig. 6b). Then $cppca^{2-}$ ligands adopting μ_2-κN,O:κO′ modes bridge Mn_3 and Mn_4 centers of the adjacent chains into a 2D corrugated layer with an irregular ring in which the two $Hcppca^-$ ligands with μ_1-κN,O coordination mode are filled and coordinated with Mn_2 centers as the terminal chelators (Fig. 6c). The $cppca^{2-}$ anions with μ_4-κN,O:κO′:κO″:κO‴ modes in 2D corrugated layers joined Mn_1 ions to generate a 3D network (Fig. 6d). From the perspective of network topology, $cppca^{2-}$ anions interacting with two Mn ions can be regarded as a line;

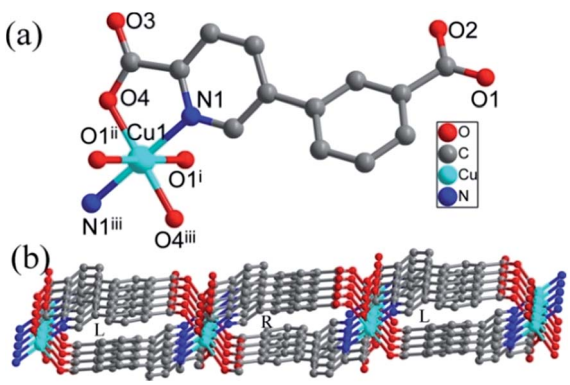

Fig. 5 (a) Coordination environment of the Cu(II) ion. The hydrogen atoms are omitted for clarity. (b) The 2D layer constructed by 1D left- and right-handed helical chains in compound **5**.

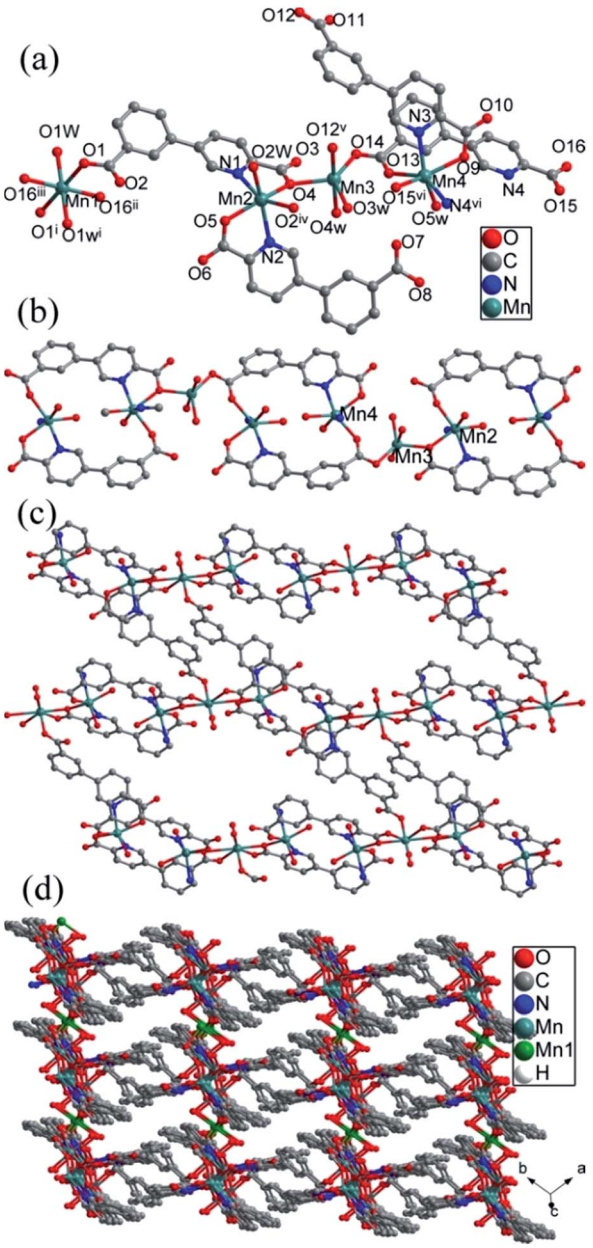

Fig. 6 (a) The coordination environments of Mn(II) centers, (b) the 1D chain constructed by Mn_3 SBUs and $cppca^{2-}$ anions, (c) the 2D layer constructed by 1D chains and μ_2-$cppca^{2-}$ anions, (d) the 3D network in compound **6**.

cppca^{2-} anion with μ_4 coordination modes interacting with two Mn_3 SBUs and Mn_1 center is regarded as a 3-connected node, hexa-coordinated Mn_1 center interacting four cppca^{2-} ligands is also a 4-connected node; linear Mn_3 SBU is considered as a 5-connected node. So the framework of compound **6** may be simplified into a 3-nodal net with Schlafli symbol $\{4^2\cdot6\}\{4^2\cdot8^2\cdot10^2\}\{4^3\cdot6^2\cdot8\cdot10^4\}_2$, which shows an unprecedented$^{3-5}$-connected topology net determined by TOPOS (Fig. 7).

Characterization

The experimental and simulated PXRD patterns of compounds **1–6** are shown in Fig. S3.† The simulated PXRD patterns from the single-crystal X-ray diffraction data are in agreement with the observed ones, indicating the phase purity of these synthesized crystalline products. The different intensities between the simulated and experimental patterns may be caused by the preferred orientation of the powder samples.

The FT-IR spectra of compounds **1–6** are displayed in Fig. 8. The wide peaks at 3445 cm^{-1} in compounds **1–6** belong to the O–H stretching. The absorption peaks located at 1605 and 1392 cm^{-1} can be ascribed to asymmetric and symmetric stretching vibrations of carboxylate groups, respectively. The peaks in the range of 1257–1032 cm^{-1} can be ascribed to the in-plane bending vibration of C–H in the benzene ring, while the out-plane bending stretching vibrations appear in the range of 762 to 694 cm^{-1}. Notably, the peak at 1058 cm^{-1} for compound **4** corresponds to the stretching vibration of P–O bonds due to the present of $[H_2P_2O_7]^{2-}$ anions.

TG curves of compounds 1–6

The thermal behaviors of compounds **1–6** were studied from 14 °C to 750 °C under air (Fig. 9). The thermogravimetric analysis (TGA) curves of compounds **1–4** and **6** have similar thermal behavior with two-step weight loss. The first weight loss corresponded to the weight loss of water molecules (obsd 26.32% for **1**, 26.38% for **2**, 10.98% for **3**, 13.31% for **4**; 8.25% for **6**; calcd 26.49% for **1**, 26.45% for **2**, 11.29% for **3**, 12.64% for **4**, 8.43% for **6**). The second weight loss of **1–4** and **6** were characteristic of the combustion of organic ligands (obsd 55.11% for **1**, 54.94% for **2**, 56.46% for **3**, 43.43% for **4**, 72.05% for **6**; calcd 55.20% for **1**, 55.16% for **2**, 56.50% for **3**, 41.06% for **4**, 71.94% for **6**). The total weight loss of compounds **1–4** and **6** amounted to 81.61%, 81.56%, 67.44%, 56.74%, 80.30%, respectively, and the remaining weight correspond to the formation of NiO, CoO, CdO, $Cd_3(PO_4)_2$, MnO (obsd 18.57% for **1**, 18.68% for **2**, 32.56% for **3**; 43.26% for **4**, 19.70% for **6**; calcd 18.31% for **1**, 18.36% for **2**, 32.21% for **3**, 46.30% for **4**, 19.63% for **6**).

The framework of compounds **5** is thermally stable up to 300 °C, on further heating, the (Hcppca)$^-$ ligand begins to rapidly decompose, the total weight loss of compounds **5** amounted to 84.95%, and the remaining weight is ascribed to the formation of CuO (obsd 15.05%, calcd 14.59%).

Luminescence property

Under UV illumination, H_2cppca ligand can't give off light, however, compounds **3** and **4** exhibit strong blue light emission. The solid-state photoluminescence behavior of H_2cppca, compounds **3** and **4** were measured at room temperature (Fig. 10). They all exhibit strong blue light emission when excited at 280 nm. The free H_2cppca and compound **3** exhibit emission bands at 396 nm and 375 nm, respectively, while

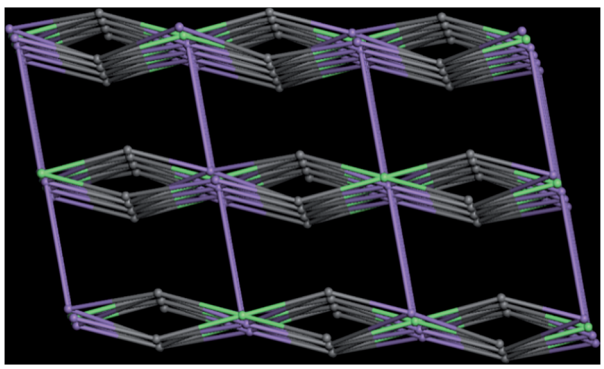

Fig. 7 The topology network of compound **6**.

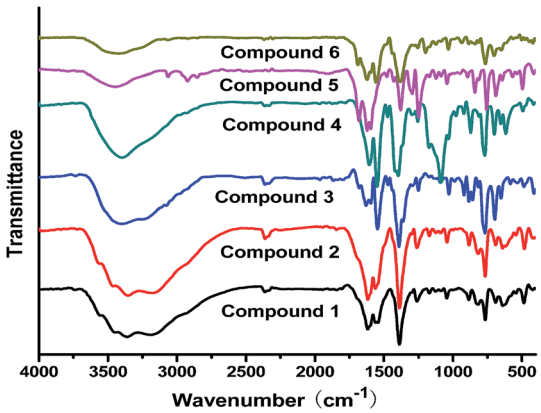

Fig. 8 The IR spectra of compounds **1–6**.

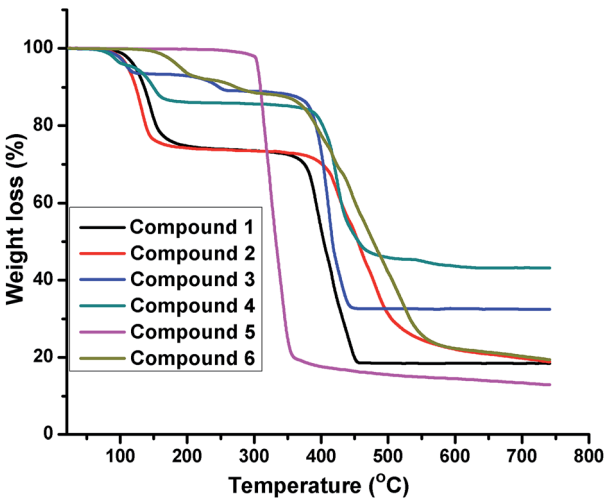

Fig. 9 The TGA curves of compounds **1–6**.

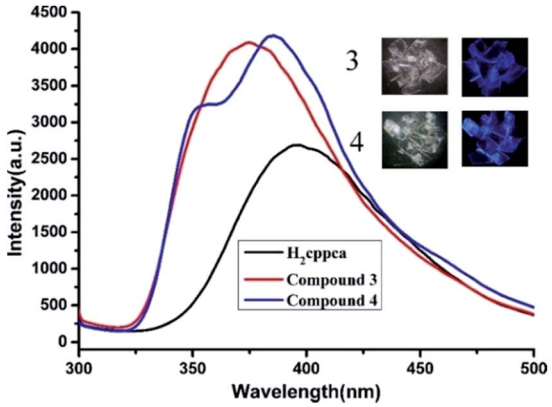

Fig. 10 Solid-state emission spectra of compounds **3** and **4** together with H_2cppca. Insets are the photo images of compounds **3** and **4** under daylight (Left) and UV illumination (Right) at 365 nm, respectively.

a blue emission band at 385 nm with a shoulder peak at 355 nm is observed in compound **4**. Compared with H_2cppca, the emission maximum of compounds **3** and **4** are slightly blue-shifted by 21 and 11 nm, respectively. So the emission bands of compounds **3** and **4** may be attributed to synergistic effects between intraligand charge transfer (LLCT) and ligand-to-metal transition (LMCT).[14] Notably, the fluorescence intensities of compounds **3** and **4** are apparently stronger than that of H_2cppca ligand under the same experimental conditions, which may be attributed to the unique coordination of ligand $cppca^{2-}$ to the Cd(II) centers increasing the conformational rigidity, thereby reducing the non-radiative energy loss.[15]

The intense blue light emission of compounds **3** and **4** encouraged us to use them as hosts for the sensing of small molecules. The ground powders of compound **3** or **4** (0.5 mg) were immersed in water and common organic solvents 4.00 mL, methanol (MeOH), ethanol (EtOH), acetonitrile (CH_3CN), *N*,*N*-dimethylformamide (DMF), *N*,*N*-dimethylacetamide (DMA), formaldehyde, cyclohexane, trichloromethane ($CHCl_3$) and acetone, then treated by ultrasonication for 0.5 hours, and the corresponding PL spectra were measured as shown in Fig. 11a. The emission spectra of compounds **3** and **4** (λ_{ex} = 280 nm) dispersed in different solvents revealed that the corresponding maximum emission peaks are largely dependent on the solvent molecules. For **3**, the emission peak with slightly shifted compared with its solid state emission spectrum (λ_{em} = 375 nm), while the maximum emission peaks for **4** have a subtle blue-shifted by 9 nm compared with its solid state emission spectrum (λ_{em} = 385 nm) (Fig. S4†). This phenomenon may be ascribed to the interactions between homogeneously dispersible framework and solvent molecules with different polarities.[16]

Notably, the fluorescent intensities of compounds **3** and **4** vary with the solvent molecules. The maximum luminescence intensity of 3-solvent emulsions gradually decreased in the order EtOH > MeOH > H_2O > DMA > CH_3CN > $CHCl_3$ > formaldehyde > cyclohexane > DMF > acetone for **3**; while for **4**, the order is EtOH > DMA > CH_3CN > DMF > cyclohexane > $CHCl_3$ > MeOH > H_2O > formaldehyde > acetone. Obviously, ethanol exhibits the most significant enhancing effect of fluorescence, while acetone exerted the significant quenching effect.

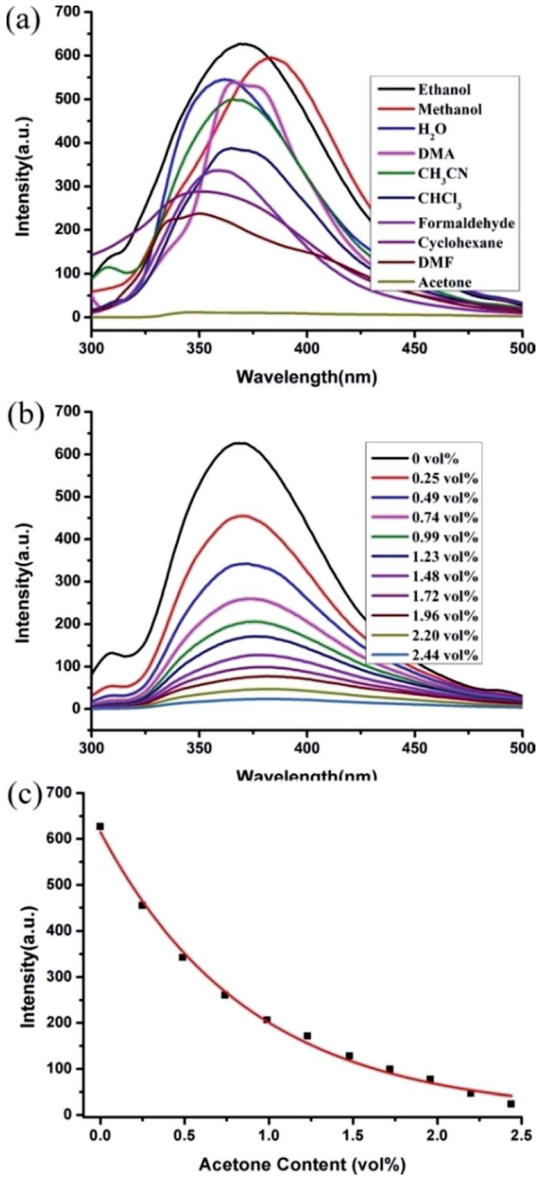

Fig. 11 (a) Emission spectra of compound **3** in different solvents when excited at 280 nm, (b) fluorescence titration of compound **3** dispersed in ethanol by gradual addition of acetone in ethanol, (c) the emission intensities of compound **3** in ethanol as a function of acetone content.

In addition, the sensing ability toward acetone for compounds **3** and **4** were further investigated. 0.5 mg samples of compounds **3** or **4** dispersed in ethanol were considered as the standard emulsion, and a batch of emulsions with gradually increased analytes concentration were prepared and monitored through fluorescent spectra. As seen in Fig. 11b, the fluorescence intensity of **3**-ethanol emulsion has a significant decrease with the increasing concentration of acetone. The fluorescence quenching percentages (QP) can be calculated using equation:[17]

$$QP = (I_0 - I)/I_0 \times 100\%$$

where, I_0 is the initial fluorescence intensity of the emulsion without the analyte, and I is the fluorescence intensity of the emulsion with the analyte. When the concentration of acetone increased to 0.49 vol%, the QP value is 45.38%, and the emission intensity was nearly disappeared with a QP of almost zero at an acetone content of 2.44 vol%. Similarly, compound **4** also features such highly sensitive and selective sensing for acetone molecules in ethanol solution (Fig. S4b†), meanwhile, 2.44 vol% acetone concentration also result in also exhibited a substantial quenching efficiency of **4**-ethonal emulsion (100%). Noticeably, the fluorescence decrease value was nearly proportional to the acetone concentration for **3** and **4**, which be well fitted with a first-order exponential decay (Fig. 11c and S4c†), indicating that the fluorescence quenching behavior for acetone of **3** or **4** is diffusion-controlled process.[18] The results reveal that compounds **3** and **4** could be promising luminescent probes for detecting acetone molecules.

In order to investigate the mechanism of quenching behavior by acetone, the UV-Vis spectra of acetone and the other solvents were measured (Fig. S5†). The results revealed that only acetone has a strong absorption ranging from 270 to 330 nm, while other solvents have no significant absorption in this range. Notably, the excitation wavelength of the compound **3** and **4** is 280 nm, which is completely overlaid by the absorbing band of acetone. Upon excitation at 280 nm, there is competition for the absorption of the light source energy between as-synthesized **3** and **4** and acetone molecules. So the efficient quenching of acetone in this system might be ascribed to the physical interaction of the solute and the solvent, which induces the changes in energy transfer.[18b,19]

Magnetic properties of compounds 1, 2, 5 and 6

Variable-temperature magnetic susceptibilities for compounds **1**, **2**, **5** and **6** were measured in the temperature range of 2–300 K under a 1000 Oe applied field. For compound **1**, the $\chi_m T$ value is 1.03 $cm^3\ mol^{-1}\ K$ at $T = 300$ K (Fig. 12), which is close to the spin-only value of 1.00 $cm^3\ K\ mol^{-1}$ for Ni(II) ($S = 1$ and $g = 2.0$). The $\chi_m T$ of **1** slightly decreases with decreasing temperature and sharply reach a minimum (0.71 $cm^3\ mol^{-1}\ K$) at 2 K. In χ_m^{-1} *versus* T curve, the magnetic susceptibilities data follow the Curie–Weiss law ($\chi_m = C/(T - \theta)$) above 20 K with Curie constant $C = 1.05\ cm^3\ K\ mol^{-1}$ and the Weiss constant $\theta = -0.15$ K. According to the formulas $C = 0.125g^2\sum S(S+1)$, the g value is 2.1 for **1**. For **2**, the $\chi_m T$ value is 2.16 $cm^3\ mol^{-1}\ K$ at $T =$ 300 K (Fig. 13), which is higher than the spin-only 1.875 $cm^3\ K\ mol^{-1}$ for Co^{II} ion (Co^{II}, $S = 3/2$ and $g = 2.0$). The $\chi_m T$ continuously decreases with decreasing temperature and reach a minimum (1.34 $cm^3\ mol^{-1}\ K$) at 2 K. In χ_m^{-1} *versus* T curve, the magnetic susceptibilities data follow the Curie–Weiss law ($\chi_m = C/(T - \theta)$) above 30 K with Curie constant $C = 2.27\ cm^3\ K\ mol^{-1}$ and the Weiss constant $\theta = -5.80$ K. According to the formulas $C = 0.125g^2\sum S(S+1)$, the g value is 2.18 for **2**. The negative value of θ and the decrease of $\chi_m T$ indicate weak antiferromagnetic interactions in compounds **1** and **2**.[20]

For compound **5** (Fig. 14), the $\chi_m T$ value is 0.389 $cm^3\ mol^{-1}$ K at $T = 300$ K, which is higher than the spin-only value of 0.375 $cm^3\ K\ mol^{-1}$ for Cu(II) ($S = 1/2$ and $g = 2.0$). Upon cooling, the $\chi_m T$ continuously decreases with decreasing temperature and reach a minimum (0.79 $cm^3\ mol^{-1}\ K$) at 2 K. In χ_m^{-1} *versus* T curve, the magnetic susceptibilities data follow the Curie–Weiss law ($\chi_m = C/(T - \theta)$) above 50 K with Curie constant $C = 1.98$ $cm^3\ K\ mol^{-1}$ and the Weiss constant $\theta = -8.11$ K. According to the formulas $C = 0.125g^2\sum S(S+1)$, the g value is 2.14 for **5**. The negative value of θ and the decrease of $\chi_m T$ indicate weak antiferromagnetic interactions between Cu(II) centers in

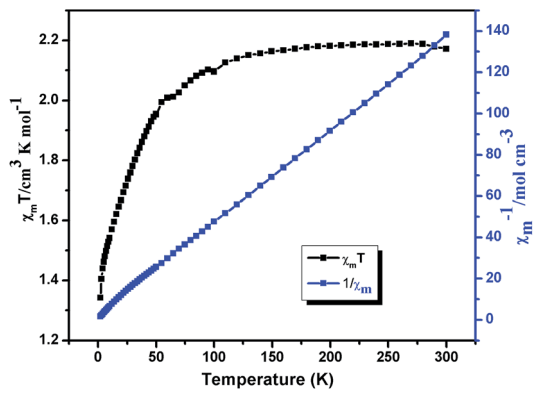

Fig. 13 Plots of $\chi_m T$ (black) and χ_m^{-1} *vs.* T (blue) for compound **2**.

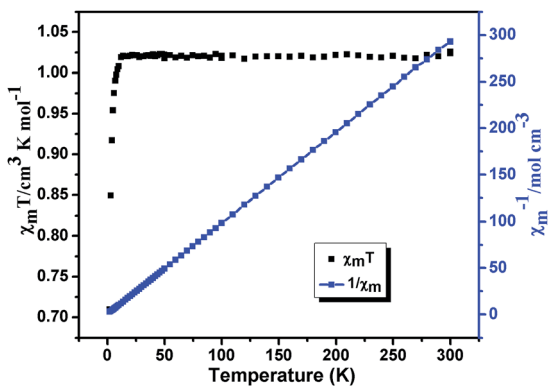

Fig. 12 Plots of $\chi_m T$ (black) and χ_m^{-1} *vs.* T (blue) for compound **1**.

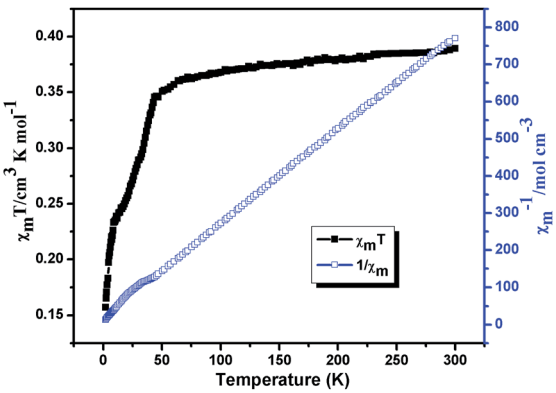

Fig. 14 Plots of $\chi_m T$ (black) and χ_m^{-1} *vs.* T (blue) for compound **5**.

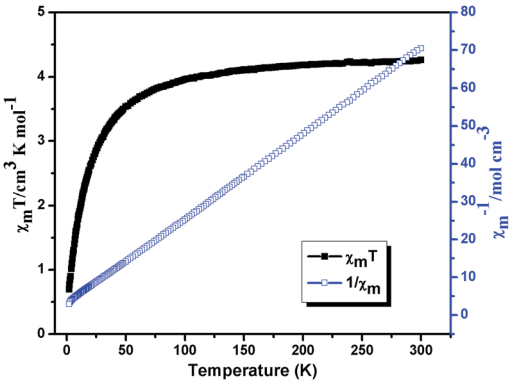

Fig. 15 Plots of $\chi_m T$ (black) and χ_m^{-1} *vs.* T (blue) for compound **6**.

compounds **5**.[21] The field dependence of the magnetization for compound **5** at 2 K in the range of −70–70 kOe shows no hysteresis loop (Fig. S6†), which indicates no 3D magnetic ordering behavior exists even at 2 K. The experimental magnetization shows an abrupt increase to 0.89 Nβ before 40 kOe and further steadily increases to 1.03 Nβ at 70 kOe, which is close to the value for one uncoupled Cu^{II} ion. This behavior further consist well with the result obtained from $\chi_m T$ *vs.* T plot, indicating that there are very weak antiferromagnetic interactions between the Cu^{2+} ions in compound **5**.

The $\chi_m T$ and χ_m^{-1} *vs.* T plots for **6** are shown in Fig. 15, the $\chi_m T$ value of Mn(II) ion at 300 K is 4.26 cm^3 K mol^{-1}, which is close to the expected value (4.38 cm^3 K mol^{-1}) for magnetically non-interacting Mn(II) ions with $S = 5/2$ and $g = 2.0$. Upon cooling, $\chi_m T$ decreases smoothly to a minimum of 0.69 cm^3 K mol^{-1} at 2 K, and the decrease of $\chi_m T$ indicates a dominant antiferromagnetic interactions among the Mn(II) centers. In χ_m^{-1} *versus* T curve, the magnetic behavior of compound **6** obeys the Curie–Weiss law ($\chi_m = C/(T - \theta)$) in the temperature range of 2–300 K, and the corresponding Curie and Weiss constants are 4.45 cm^3 K mol^{-1} and −13.43 K (θ), respectively. According to the formulas $C = 0.125g^2\sum S(S + 1)$, the g value is 2.02. The large negative θ value further indicates significant antiferromagnetic interactions exist between neighboring Mn(II) ions.[20,22]

Conclusion

In summary, six new coordination compounds based on H_2cppca ligand have been synthesized and characterized in detail. Compounds **1–6** have rich structural chemistry ranging from mononuclear (**1** and **2**), one-dimensional (**3** and **4**), two-dimensional (**5**) to three-dimensional (**6**) structures. Moreover, the framework of compound **6** may be simplified into a 3-nodal net with Schlafli symbol $\{4^2\cdot6\}\{4^2\cdot8^2\cdot10^2\}\{4^3\cdot6^2\cdot8\cdot10^4\}_2$, which shows an unprecedented[3–5]-connected topology net. Compounds **3** and **4** show efficiently and easily recycled fluorescent probes for the acetone molecules. Weak antiferromagnetic interactions were observed in compounds **1**, **2**, **5** and **6**. The further research for the construction of new coordination compounds based on H_2cppca ligand is underway in our laboratory.

Acknowledgements

This work was supported by the National Natural Science Foundation of China (No. 21201155), the Natural Science Young Scholars Foundation of Shanxi Province (No. 2012021007-5 and 2013021008-6), Program for the Top Young Academic Leaders of Higher Learning Institutions of Shanxi and 131 Talent Plan of Higher Learning Institutions of Shanxi, respectively.

Notes and references

1 (*a*) S. R. Batten and R. Robson, *Angew. Chem., Int. Ed.*, 1998, **37**, 1460; (*b*) L. Carlucci, G. Ciani and D. M. Proserpio, *Coord. Chem. Rev.*, 2003, **246**, 247; (*c*) A. Harada, A. Hashidzume, H. Yamaguchi and Y. Takashima, *Chem. Rev.*, 2009, **109**, 5974; (*d*) G. E. Kostakis, A. M. Ako and A. K. Powell, *Chem. Soc. Rev.*, 2010, **39**, 2238; (*e*) R. Chakrabarty, P. S. Mukherjee and P. J. Stang, *Chem. Rev.*, 2011, **111**, 6810; (*f*) D. Zhao, D. J. Timmons, D. Q. Yuan and H. C. Zhou, *Acc. Chem. Res.*, 2011, **44**, 123; (*g*) J. Yang, J. F. Ma and S. R. Batten, *Chem. Commun.*, 2012, **48**, 7899; (*h*) L. Carlucci, G. Ciani, D. M. Proserpio, T. G. Mitina and V. A. Blatov, *Chem. Rev.*, 2014, **114**, 7557.

2 (*a*) A. M. Seayad and D. M. Antonelli, *Adv. Mater.*, 2004, **16**, 765; (*b*) J. L. C. Rowsell and O. M. Yaghi, *Angew. Chem., Int. Ed.*, 2005, **44**, 4670; (*c*) V. V. Struzhkin, B. Militzer, W. L. Mao, H.-k. Mao and R. J. Hemley, *Chem. Rev.*, 2007, **107**, 4133; (*d*) J. R. Li, R. J. Kuppler and H. C. Zhou, *Chem. Soc. Rev.*, 2009, **38**, 1477; (*e*) A. Phan, C. J. Doonan, F. J. Uribe-Romo, C. B. Knobler, M. O'Keeffe and O. M. Yaghi, *Acc. Chem. Res.*, 2010, **43**, 58; (*f*) G. Ferey, C. Serre, T. Devic, G. Maurin, H. Jobic, P. L. Llewellyn, G. De Weireld, A. Vimont, M. Daturi and J. S. Chang, *Chem. Soc. Rev.*, 2011, **40**, 550; (*g*) J. Canivet, A. Fateeva, Y. Guo, B. Coasne and D. Farrusseng, *Chem. Soc. Rev.*, 2014, **43**, 5594; (*h*) B. Van de Voorde, B. Bueken, J. Denayer and D. De Vos, *Chem. Soc. Rev.*, 2014, **43**, 5766; (*i*) Q. Wang, J. Bai, Z. Lu, Y. Pan and X. You, *Chem. Commun.*, 2016, **52**, 443.

3 (*a*) L. E. Kreno, K. Leong, O. K. Farha, M. Allendorf, R. P. V. Duyne and J. T. Hupp, *Chem. Rev.*, 2012, **112**, 1105; (*b*) X. Sun, Y. Wang and Y. Lei, *Chem. Soc. Rev.*, 2015, **44**, 8019; (*c*) J. Wu, B. Kwon, W. Liu, E. V. Anslyn, P. Wang and J. S. Kim, *Chem. Rev.*, 2015, **115**, 7893; (*d*) L. You, D. Zha and E. V. Anslyn, *Chem. Rev.*, 2015, **115**, 7840; (*e*) X. Zhou, S. Lee, Z. Xu and J. Yoon, *Chem. Rev.*, 2015, **115**, 7944.

4 (*a*) M. Kurmoo, *Chem. Soc. Rev.*, 2009, **38**, 1353; (*b*) M. Murrie, *Chem. Soc. Rev.*, 2010, **39**, 1986; (*c*) G. Rogez, N. Viart and M. Drillon, *Angew. Chem., Int. Ed.*, 2010, **49**, 1921; (*d*) M. Clemente-Leon, E. Coronado, C. Marti-Gastaldo and F. M. Romero, *Chem. Soc. Rev.*, 2011, **40**, 473; (*e*) X. Y. Wang, C. Avendano and K. R. Dunbar, *Chem. Soc. Rev.*, 2011, **40**, 3213; (*f*) D. F. Weng, Z. M. Wang and S. Gao, *Chem. Soc. Rev.*, 2011, **40**, 3157; (*g*) J. Yuan, Y. Xu and A. H. Muller, *Chem. Soc. Rev.*, 2011, **40**, 640; (*h*) J. Tao, R. J. Wei, R. B. Huang and L. S. Zheng, *Chem. Soc. Rev.*, 2012, **41**, 703.

5 (*a*) J. Lee, O. K. Farha, J. Roberts, K. A. Scheidt, S. T. Nguyen and J. T. Hupp, *Chem. Soc. Rev.*, 2009, **38**, 1450; (*b*) A. Corma, H. Garcıa and F. X. LlabresiXamena, *Chem. Rev.*, 2010, **110**, 4606; (*c*) A. Dhakshinamoorthy and H. Garcia, *Chem. Soc. Rev.*, 2014, **43**, 5750; (*d*) J. W. Liu, L. F. Chen, H. Cui, J. Y. Zhang, L. Zhang and C. Y. Su, *Chem. Soc. Rev.*, 2014, **43**, 6011; (*e*) A. Dhakshinamoorthy, A. M. Asiri and H. Garcia, *Chem. Soc. Rev.*, 2015, **44**, 1922.

6 (*a*) N. W. Ockwig, O. Delgado-Friedrichs, M. O'Keeffe and O. M. Yaghi, *Acc. Chem. Res.*, 2005, **38**, 176; (*b*) A. K. Cheetham, C. N. R. Rao and R. K. Feller, *Chem. Commun.*, 2006, **46**, 4780; (*c*) I. G. Georgiev and L. R. MacGillivray, *Chem. Soc. Rev.*, 2007, **36**, 1239; (*d*) O. K. Farha and J. T. Hupp, *Acc. Chem. Res.*, 2010, **43**, 1166; (*e*) N. Stock and S. Biswas, *Chem. Rev.*, 2012, **112**, 933; (*f*) M. O'Keeffe and O. M. Yaghi, *Chem. Rev.*, 2012, **112**, 675; (*g*) N. Stock and S. Biswas, *Chem. Rev.*, 2012, **112**, 933; (*h*) C. Wang, T. Zhang and W. Lin, *Chem. Rev.*, 2012, **112**, 1084; (*i*) Y. Han, J. R. Li, Y. Xie and G. Guo, *Chem. Soc. Rev.*, 2014, **43**, 5952; (*j*) Z. Zhang and M. J. Zaworotko, *Chem. Soc. Rev.*, 2014, **43**, 5444; Y. X. Sun and W. Y. Sun, *Chin. Chem. Lett.*, 2014, **25**, 823.

7 (*a*) F. A. Paz, J. Klinowski, S. M. Vilela, J. P. Tome, J. A. Cavaleiro and J. Rocha, *Chem. Soc. Rev.*, 2012, **41**, 1088; (*b*) C. Zhang, M. Zhang, L. Qin and H. Zheng, *Cryst. Growth Des.*, 2014, **14**, 491; (*c*) D. Zhao, D. J. Timmons, D. Yuan and H. C. Zhou, *Acc. Chem. Res.*, 2010, **44**, 123; (*d*) X. L. Zhao and W. Y. Sun, *CrystEngComm*, 2014, **16**, 3247.

8 (*a*) Y. X. Sunand and W. Y. Sun, *CrystEngComm*, 2015, **17**, 4045; (*b*) L. Sun, J. F. Song, R. S. Zhou, J. Zhang, L. Wang, K. L. Cui and X. Y. Xu, *J. Coord. Chem.*, 2014, **67**, 822; (*c*) J. F. Song, Y. Li, R. S. Zhou, J. Shao, L. Wang and X. B. Cui, *J. Coord. Chem.*, 2015, **68**, 3651; (*d*) B. B. Shi, Y. H. Zhong, L. L. Guo and G. Li, *Dalton Trans.*, 2015, **44**, 4362.

9 (*a*) W. X. Yin, Y. T. Liu, Y. J. Ding, Q. Lin, X. M. Lin, C. L. Wu, X. D. Yao and Y. P. Cai, *CrystEngComm*, 2015, **17**, 3619; (*b*) Q. F. Li, D. Yue, G. W. Ge, X. D. Du, Y. C. Gong, Z. L. Wang and J. H. Hao, *Dalton Trans.*, 2015, **44**, 16810; (*c*) J. J. Hou, X. Q. Li, B. Q. Tian and X. M. Zhang, *CrystEngComm*, 2016, **18**, 2065; (*d*) D. S. Deng, H. Guo, G. H. Kang, L. F. Ma, X. He and B. M. Ji, *CrystEngComm*, 2015, **17**, 1871.

10 (*a*) B. M. Ji, D. S. Deng, L. F. Ma, H. L. Li, X. S. Fan, G. R. Qu, L. Cao and L. Zhou, *CrystEngComm*, 2013, **15**, 4107; (*b*) J. Cepeda, S. Pérez-Yáñez, G. Beobide, O. Castillo, A. Luque, P. A. Wright, S. Sneddon and S. E. Ashbrook, *Cryst. Growth Des.*, 2015, **15**, 2352; (*c*) R. G. AbdulHalim, A. Shkurenko, M. H. Alkordi and M. Eddaoudi, *Cryst. Growth Des.*, 2016, **16**, 722.

11 (*a*) B. M. Ji, D. S. Deng, X. He, B. Liu, S. B. Miao, N. Ma, W. Z. Wang, L. G. Ji, P. Liu and X. F. Li, *Inorg. Chem.*, 2012, **51**, 2170; (*b*) L. B. Hamdy, P. R. Raithby, L. H. Thomas and C. C. Wilson, *New J. Chem.*, 2014, **38**, 2135.

12 (*a*) J. Xiao, B. Y. Liu, G. Wei and X. C. Huang, *Inorg. Chem.*, 2011, **50**, 11032; (*b*) S. W. Zhang, J. G. Ma, X. P. Zhang, E. Y. Duan and P. Cheng, *Inorg. Chem.*, 2015, **54**, 586.

13 G. M. Sheldrick, *Acta Crystallogr., Sect. A: Found. Crystallogr.*, 2008, **64**, 112.

14 (*a*) F. Y. Yi, Y. Wang, J. P. Li, D. Wu, Y. Q. Lan and Z. M. Sun, *Mater. Horiz.*, 2015, **2**, 245; (*b*) F. Y. Yi, J. P. Li, D. Wu and Z. M. Sun, *Chem.–Eur. J.*, 2015, **21**, 11475; (*c*) Y. L. Wu, G. P. Yang, Y. Q. Zhao, W. P. Wu, B. Liu and Y. Y. Wang, *Dalton Trans.*, 2015, **44**, 3271; (*d*) W. H. Huang, J. Z. Li, T. Liu, L. S. Gao, M. Jiang, Y. N. Zhang and Y. Y. Wang, *RSC Adv.*, 2015, **5**, 97127.

15 (*a*) Y. Y. Wang, Q. Jin, S. X. Liu, C. Guo, Y. Y. Liu, B. Ding, X. X. Wu, Y. Li and Z. Z. Zhu, *RSC Adv.*, 2015, **5**, 35238; (*b*) S. S. Chen, Z. S. Bai, J. Fan, G. C. Lv, Z. Su, M. S. Chen and W. Y. Sun, *CrystEngComm*, 2010, **12**, 3091.

16 (*a*) S. R. Zhang, D. Y. Du, J. S. Qin, S. J. Bao, S. L. Li, W. W. He, Y. Q. Lan, P. Shen and Z. M. Su, *Chem.–Eur. J.*, 2014, **20**, 3589; (*b*) L. L. Wen, X. F. Wang, H. Shi, K. L. Lv and C. G. Wang, *RSC Adv.*, 2016, **6**, 1388; (*c*) S. Pramanik, Z. C. Hu, X. Zhang, C. Zheng, S. Kelly and J. Li, *Chem.–Eur. J.*, 2013, **19**, 15964; (*d*) Y. X. Zhu, Z. W. Wei, M. Pan, H. P. Wang, J. Y. Zhang and C. Y. Su, *Dalton Trans.*, 2016, **45**, 943; (*e*) M. J. Zhang, H. X. Li, H. Y. Lia and J. P. Lang, *Dalton Trans.*, 2016, **45**, 17759.

17 Z. M. Ju, W. Yan, X. J. Gao, Z. Z. Shi, T. Wang and H. G. Zheng, *Cryst. Growth Des.*, 2016, **16**, 2496.

18 (*a*) F. H. Liu, C. Qin, Y. Ding, H. Wu, K. Z. Shao and Z. M. Su, *Dalton Trans.*, 2015, **44**, 1754; (*b*) J. A. Hua, Y. Zhao, Y. S. Kang, Y. Lu and W. Y. Sun, *Dalton Trans.*, 2015, **44**, 11524; (*c*) Z. Y. Guo, H. Xu, S. Q. Su, J. F. Cai, S. Dang, S. C. Xiang, G. D. Qian, H. J. Zhang, M. O'Keeffe and B. L. Chen, *Chem. Commun.*, 2011, **47**, 5551.

19 (*a*) S. T. Zhang, J. Yang, H. Wu, Y. Y. Liu and J. F. Ma, *Chem.–Eur. J.*, 2015, **21**, 15806; (*b*) Z. M. Hao, X. Z. Song, M. Zhu, X. Meng, S. N. Zhao, S. Q. Su, W. T. Yang, S. Y. Song and H. J. Zhang, *J. Mater. Chem. A*, 2013, **1**, 11043; (*c*) Q. Liu, J. M. Yang, F. Guo, L. N. Jin and W. Y. Sun, *Dalton Trans.*, 2016, **45**, 5841.

20 (*a*) R. Patra, H. M. Titi and I. Goldberg, *CrystEngComm*, 2013, **15**, 2863; (*b*) R. Patra, H. M. Titi and I. Goldberg, *CrystEngComm*, 2013, **15**, 7257.

21 S. X. Cui, Y. L. Zhao, J. P. Zhang, Q. Liu and Y. Zhang, *Cryst. Growth Des.*, 2008, **8**, 3803.

22 F. W. Zhang, Z. F. Li, T. Z. Ge, H. C. Yao, G. Li, H. J. Lu and Y. Y. Zhu, *Inorg. Chem.*, 2010, **49**, 3776.

